FORMULATION AND EVALUATION OF DNA NANOCLEWS FOR STIMULI RESPONSIVE 5-FLUOROURACIL ANTICANCER DRUG BY ROLLING CIRCLE AMPLIFICATION METHOD

Mr. Rahul Jain[1]*, Dr. Namrata Singh[2]

Received: 27/09/21 Revised : 28/10/21 Accepted: 08/11/21 Published: 30/11/21

Abstract:
Rolling circle amplification (RCA) has recently emerged as a potent way for producing regularly organised DNA structures, in addition to its long-established ability to improve biological signals. The method for producing nano-scaled cocoon-like DNA particles, nicknamed DNA nanoclews, for transporting and distributing tiny amounts of chemotherapeutic drug is presented here. The researchers were able to control the timing and location of drug discharge by encapsulating the DNA-degrading enzyme DNase I in a polymeric nanogel. Using endosomal acidity as a trigger, this clever drug delivery system based on RCA amplicons may penetrate specific cells and release the payload.

Keywords: 5-Fluorouracil, DNA, Nanoclew, Rolling circle amplification.

[1*,2]Department of Pharmacy, Oriental University, Sanwer Road, Opp. Rewati Range Indore (M.P)

***Corresponding Author:** Mr. Rahul Jain
*Department of Pharmacy, Oriental University, Sanwer Road, Opp. Rewati Range, Indore (M.P) (rahulkjain87@gmail.com)

DOI: 10.53555/ecb/2021.10.4.27

1. Introduction

The dissemination of medication or Drug Delivery Systems (MDSs / DDSs) was hindered due to physiological limitations that impeded the efficiency and speed of medication delivery (1) (2) (3). Device and formulation (4) (5), based drug delivery systems (DDSs) were developed to respond to the physiological properties of diseases to enhance the pharmacokinetics and pharmacodynamics of drugs (6) (7) (8). During this time, a large number of articles in a variety of academic areas have been published as a consequence of substantial DDS research. (9) (10) (11). DDSs have transformed throughout the last 6 decades, and they may be classified into three categories (12) (13). Early strategies for prolonged medication delivery (dating back to the 1950s) have been established as oral formulations or patches for transdermal application. (14). During this period, fundamental drug dispersion principles such as dispersion, disintegration, osmosis, and the exchange of ions started to emerge. (15). The second generation of controlled release is a strategy that has been successfully employed from the 1980s to keep medicine concentrations consistent in the circulatory system. (16) (17). There hadn't been numerous second generation DDSs on the marketplace before this time frame began. (18), However, during this time period, the invention of bio-responsive polymers created room for simpler to manage DDSs. (19). Starting roughly the year 2010, an additional generation of DDSs constructed from nanostructures with flexible and adaptable physiochemical qualities (20) for promoting the principle of "precision medicines" have been developed. (21) (22) (23), individualized genomes insights will be utilized to adjust the administration of drugs as well as enhance bioavailability. (24) (25) (26) (27). We are going to start with our investigation by offering a complete review of the medication distributing industry, focusing on the key components that influence why, what, and how medications are distributed. This is carried out in order to enhance the success rate of the treatment. Following that, utilizing carcinoma as model ailments, the focus will be on nanocarriers, perhaps the most contemporary drug delivery methodology, to show the physiologic hurdles and accompanying strategies for precise administration of medicines. Emerging suggestions for developing "intelligent" nanomedicine, which is such as ways to use physiologically inputs to manage nanocarrier targeted and releasing characteristics such as faster cellular absorption or stimuli-responsive release of medications, will also be addressed. Insights acquired through FDA approved nano-formulations and formulations which are currently being studied in clinical trials are additionally given.

2. Designing Criteria of Nanocarriers for Drug Delivery

Due to the numerous hurdles on their path from the injection to the desired location, only a small proportion of those "lucky" nanocarriers arrive at their destination. Because of breakthroughs in material science, researchers may now accurately modify the qualities of nanocarriers in terms of material composition, size, shape, and surface features (28). To help you construct efficient nanocarriers, we've provided ideal values for these features below:

2.1 Size

To construct nano-particulate carriers for drug administration, size is the most important characteristic to manage within an ideal range. To avoid the difficulty of form, we will examine the size preferences of nanocarriers for anticancer therapy using a spherical nanocarrier as a model. Too tiny nanocarriers (less than 10 nm) are quickly removed from the circulation by glomerular filtration (29), Due to the limiting diameter of the capillaries (µ5 m), nanocarriers that are excessively big (> 2 µm) likely to block the blood vessels (30). The dimensions of tumor-targeted nanocarriers ought to be tailored to satisfy the EPR effect, which limits particle size to 500 nm or greater and prefers particles larger than 200 nm (31). Nanotransporters bigger than 200 nm are also at danger of being cleared by other organs such as the liver, spleen, or lung, which reduces their circulation half-time. In addition to tumour buildup, the capacity of nanocarriers in the sub-100 nm range to penetrate thick solid tumours makes them more effective carriers. A systematic study of mono-dispersed silica-based nanocarriers of three different sizes (20 nm, 50 nm, and 200 nm) revealed that nanocarriers of 50 nm diameter had the highest tumour accumulation and penetration efficacies, outperforming nanocarriers near the lower and upper size limits. Overall, nanocarriers with dimensions ranging from 10 to 200 nm, preferably less than 100 nm (32), are typically suitable for tumor targeted drug delivery.

2.2 Shape

Emerging research on the role of nanocarrier geometries revealed that shape may have a

significant impact on transport efficacy in numerous domains of the delivery process, including circulation, extravasation, and internalisation by targeted cells. Nanospheres, nanodiscs, nanorods, and nanocylinders are among the most extensively researched geometries. In terms of circulation, cylindrical or disc-like nanocarriers displayed distinct hemodynamic patterns when compared to spherical ones; circulation half-time may be extended by orienting the nanocarrier to follow blood flow or tumbling in the blood vessels. In addition, the form of the nanocarriers influences macrophage recognition, which influences bio-distribution patterns. For targeted internalisation by cancer cells, nanocarriers with a bacterium-like rod shape, such as gold nanorods and silicon nanorods, outperform their spherical counterparts, owing to the evolved machinery in human cells against bacteria. Shape, in particular, has been proven to surpass spherical nanocarriers in terms of drug delivery efficacy, making shape a crucial feature to consider while optimising nanocarriers. Emerging techniques that employ morphologically transformable nanocarriers have been proven to fully capitalise on the advantages of morphologies for enhanced drug delivery (33). A nanocarrier that can change from nonodisks to nanospheres in response to environmental cues such as pH or toxins, for example, may use the elliptical disc shape to escape macrophages and the spherical shape for internalisation (34).

To overcome the successive physiological hurdles for precise drug administration, the properties of the nanocarrier might be modified modularly in terms of size, material composition, shape, surface chemistry, and targeted ligand conjugation.

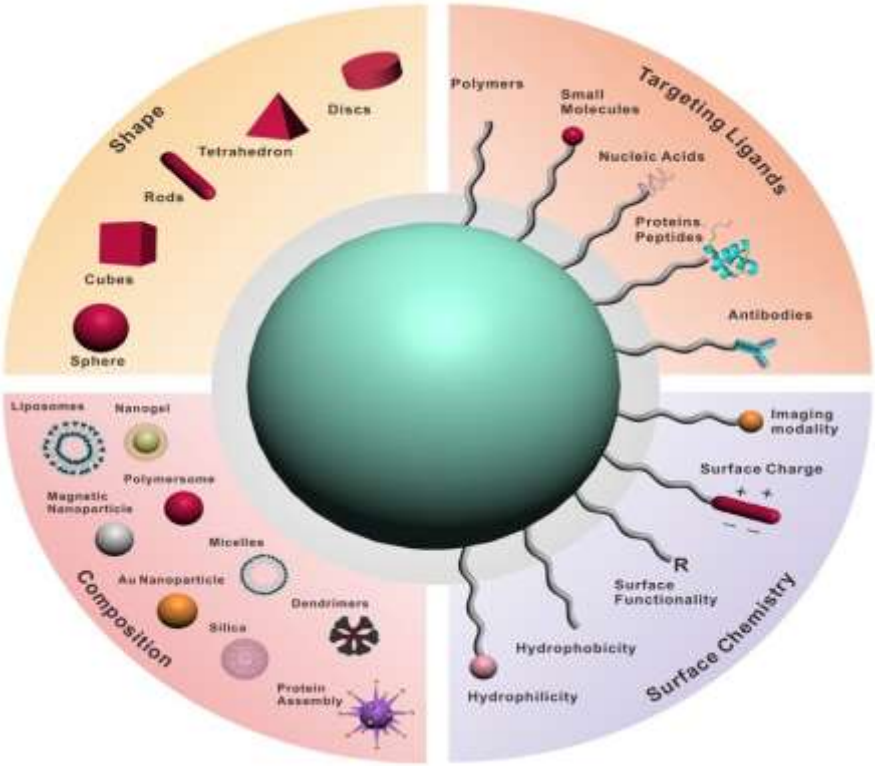

Figure 1. Design Parameters for Nanoformulations

2.3 Surface Charge

Because cell membranes are negatively charged, positively charged nanocarriers often outperform negatively charged or neutral nanocarriers in-vitro. This phenomenon occurs in a wide range of cell lines, including macrophages and cancer cells. Positively charged nanocarriers were often endocytosed via the clathrin-dependent route, whilst negatively charged nanoparticles were internalised via the caveolae-mediated pathway (35). For in-vivo injection, however, the positively charged nanocarriers may readily draw negatively charged serum proteins, creating a protein corona and raising the possibility of immune cell clearance. Additionally, the strong positive charge may cause hemolysis and platelet instability. Therefore, for long term circulation, negatively charged or neutral nanocarriers are preferred. Many nano-particulate systems have used a common strategy known as "charge-reversal" to combine the need for longer circulation with greater cellular absorption. In

order to do this, the nanocarriers were designed to remain neutral or just barely negatively charged while in motion but switch to a positive charge once they reached the tumour microenvironment. Typically, the positively charged cores' negatively charged shells are shed as a result of the acidic extra-tumoral microenvironment (36); or altering a synthetic peptide's charge such that the isoelectric point may be tweaked (37).

2.4 Surface composition

Since the nanocarriers' surfaces are where cells first come into touch with them, interactions between surface elements and cells will determine how the delivery process turns out. For instance, the hydrophobicity or hydrophilicity of the surface may have a substantial impact on cellular internalisation, and hydrophobic nanocarriers may be readily internalised (38). In this case, the hydrophilicity and circulation times of the surfaces are greatly increased using the standard PEGylation approach. Utilising naturally occurring cell membranes or coating the surface of the nanocarriers with self-markers like factor H or CD_{47} have been proposed as alternatives to PEGylation to further reduce the risk of being removed by the complement system (39) (40). In addition to impeding macrophage recognition, the presence or absence of targeting ligands on nanocarrier surfaces may influence their adherence and penetration into cancer cells. Due to the overexpressed receptors on tumours as well as vascular proximal endothelial cells, targeting ligands is a desirable component for targeted distribution with improved precision. However, it's crucial to keep in mind that healthy cells also carry cancer cell receptors, albeit to a lesser extent (41). There is still substantial harm caused by the targeted ligand.

2.5 Elasticity and degradation

Another characteristic that might be adjusted to improve delivery effectiveness is the nanocarriers' elastic properties. It has been shown that rigid nanoparticles are simpler for cells to absorb because the energy required for cell membranes to wrap up a nanoparticle reduces as stiffness increases. When injected in-vivo, stiff nanocarriers are quickly flushed out. Compared to red blood cells (RBC), elastic nanocarriers perform better in terms of circulation (42), Where the flexible RBC was easily twisted to pass through increasingly smaller diameter blood conduits. Therefore, improving the flexibility of the nanocarriers is a straightforward way to improve the circulation of the nanoparticles. When creating nanocarriers, biodegradability is an important consideration from the perspectives of both biocompatibility and the effectiveness of drug delivery. Effective drug delivery requires strategies to maintain the medicine in the carrier during circulation but release it once it reaches the target because the nanocarrier must disintegrate or dissociate in order to release the drug that has been encapsulated (43). By incorporating functional moieties into the nanocarriers that may be destroyed by certain signals in the tumour microenvironment, the medicine release in this case might be controlled. To solve the issue of biocompatibility, it is preferable to use nanomaterials that can be broken down into non-toxic chemicals. It would be great if non-degradable nanocarriers, such as those with metallic bases, could be removed from the body after serving their purpose as a delivery vehicle. By combining biodegradable DNA with metallic nanocarriers, Chan and colleagues have demonstrated a solution to the issue of making the nano-assembly dissociable into smaller nanocarriers for clearance (44).

Designing nanocarriers for effective medication delivery requires taking into account a variety of physiologic factors and combining them into a single formulation. The preparation of "smart" formulations that can use the physiological signals in the sick tissue for regulated release of medicines will be covered in more detail in the section after this one.

2.6 Smart Drug Delivery Systems Mediated by Physiological Signals

In order to allow nanocarrier-mediated drug delivery with improved spatial-temporal precision, bio-inspired strategies that provide the delivery vehicles the ability to interact with physiological environment and determine when and where to release the payload are gaining interest. These "smart" formulations were developed employing moieties that respond to stimuli and translate physiological cues from the tumour microenvironment into activities of the nanocarriers such swelling, degradation, morphological change, and charge reversal. The potential for increased anticancer efficacy of nanomedicine sensitive to physiological cues, such as acidic pH, overexpressed enzymes, redox gradient, or high metabolite concentrations, is enormous. They might have superior tumour targeting efficacies, where a larger proportion of the injected medication would be deposited in the targeted cells, and better pharmacokinetic profiles with less worry about early drug leakage during

circulation.

3. Nanoclew Drug Delivery Systems

Traditional chemotherapy, which uses anticancer medications to treat cancer, partially eliminates noncancerous cells in addition to cancer cells. Additionally, cancer cells may become resistant to treatments during drug therapy as a result of genetic mutations and changes to signalling pathways. Multidrug treatment has been given to treat the condition by focusing on several cellular pathways in order to overcome resistance to single-drug therapy. It has been shown that pharmacological combinations that target many biological pathways function better than single-drug therapy. Unfortunately, long-term therapy with several drug targets was unable to successfully cure malignancies due to the development of cancer cell resistance to multidrug therapy. Consequently, delivering therapeutic molecules for targeting various illnesses is a big problem for the traditional form of medication treatment because of the lack of selectivity, poor distribution, and confined therapeutic profiles in cancer drug therapy. The concept of a drug delivery system has advanced significantly during the last few decades (45) (46) (47) (48).

Despite the availability of other drug delivery methods, the pharmaceutical business and pharmacological researchers appear to be concentrating on the nanoclew drug delivery method for a number of reasons, including:

1. Defeating medication resistance and protecting against deterioration.
2. Increased drug bioavailability
3. Can be directed against certain tissues, cells, or organs

3.1 Properties of nanoclews

1. The following requirements must be satisfied in order to make nanoclews (NCl):
2. The NCl must successfully bind to and transport the drug(s).
3. The NCl must to be biocompatible with the body and stable in circulation.
4. To maximise its anticancer effects on tumour cells, the NCl should ideally have a high bioavailability.
5. The NCl must be able to selectively target cancer cells and avoid normal cells.
6. The drug(s) must only be released by the NP after it has reached the tumour.

Nanoclews (NCl), technically speaking, are defined as materials with a diameter of less than 100 nm and larger than 1 nm. These qualities may be attained based on the size, shape, and composition of the NCl.

3.2 Advantages of nanoclews:

1. Nanoclews' particle size and surface properties may be easily changed to produce medication targeting that is both passive and active following parenteral injection.
2. They are site-specific, non-toxic, and biodegradable.
3. Drugs can be integrated into the systems with a high drug loading and without causing any chemical reactions, which is crucial for maintaining the drug's activity.
4. They provide easily modulable particle degrading properties and a regulated rate of medication release.
5. By using magnetic guidance or adding targeted ligands to the surface of particles, they may direct a medicine to a particular location in the body.
6.They provide superior overall pharmacological response/unit dosage and therapeutic efficacy.

3.3 Disadvantages:

1. Tough to produce on a wide scale.
2. Physical handling of nanoclews in liquid and dry forms is challenging due to their tiny particle size and vast surface area, which can lead to particle-particle aggregation.
3. Limited drug loading and burst release are easily produced by small particle size and vast surface area.

4. Nanomedicine Responsive to Physiological Triggers

4.1 Acidic environment

A reliable signal to start the drug release from the DDSs is a local decrease in pH in various tissues (such as the GI tract and vagina), subcellular compartments (such as the endosome and lysosome), or disease-related conditions (such as infection, inflammation, and tumour microenvironment). Lactic acid builds up in tumours as a result of aberrant metabolic processes, such as an accelerated rate of glycolysis and inadequate lymphatic drainage. When tumor-targeted nanocarriers extravasate from the blood circulation (pH 7.4) to the extracellular space of tumours (pH 6-7.2), their pH will slightly shift. Endosomes (pH 5.0–6.0) and lysosomes (pH 4.0–5.0) will experience a further pH fall as a result of nanocarriers internalised into intracellular space (49). Numerous pH-responsive formulations have been created based on two processes to take advantage of the pH gradient:

4. Including protonatable polymers that could enable solubility or conformational changes in response to acid stimulation;
5. Using acid-cleavable bonds (like hydrazine, acetal, and ester) or acid-labile moieties (like bicarbonate salts) to enable disruption of the nanocarrier in acidic environments (50).

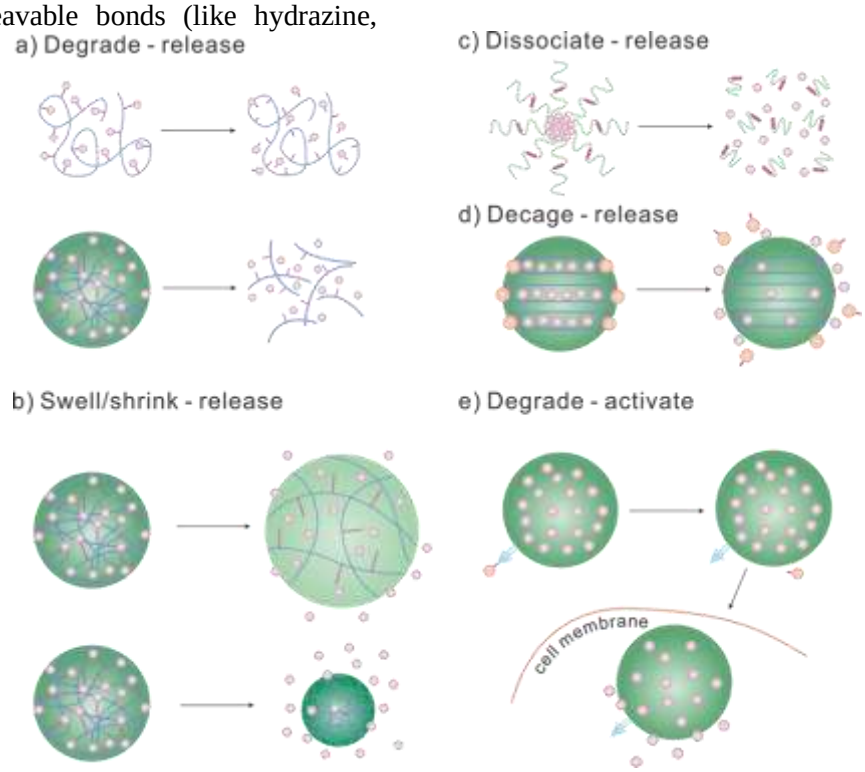

Figure 2: Mechanisms of Stimuli-responsive Nanocarrier for Drug Delivery

When a physiological signal is activated, the medicines may release from the nanocarrier.

1. degradation,
2. swell or shrink,
3. dissociation,
4. uncapping the pores of mesoporous silica nanoparticles.
5. Nanocarrier activation for cell penetration with exposed moieties.

The small pH variation that exists between the bloodstream and the extracellular environment of malignancies is often utilised as a cue for activating the nanocarriers for better tumour permeation or cancer cell internalisation, which includes shedding the stealth coating, demonstrating the cell penetrating peptide, or changing the surface charge. As an example, layer-by-layer deposition with a sheddable layered covering was used to generate an acidity-triggered internalisation in-vivo nanocarrier (51). The positively charged inner layer of the PLL was supplemented with PEG to provide a stealth layer. The amended linker was iminobiotin, and the additional linker was neutravidin. In alkaline circumstances (PH 8–12), the link is robust, while in acidic settings (PH 4–16), it disintegrates fast. By utilising PEG to mask the positive charge of the PLL, this may help lower the danger of "non-specific absorption" during circulation. However, as iminobiotine and neutravidine accumulate within the tumour, their ability to interact with one another is hampered by exposure to the acidic environment of the tumour, which leaves the positively charged layer of the PLL more vulnerable to cellular absorption. Researchers were able to increase the quantity of anticancer genes that could be given by using the PEG backbone of the polymer, which is composed of amino acids (Glu, histidine), and amino acids (His). This polymer, often referred to as poly(PEG - His-Glu), may vary its capacity for charge reversal in a pH-dependent manner (52). The charge behaviour of the nano-formulation is governed by the interaction of the polyelectrolyte, which is composed of negatively charged DNA and positively charged PEI. Because amino acids may be protonated in an acidic environment, the charge of the charge-reversible nano-carrier can shift from negative to positive. The researchers were able to improve the intracellular absorption of the nano-carrier by adjusting the ratio of these three components. They also discovered that the acid-dependence of the absorption profile for the charge-refrigerated nanocarrier differed from that

of the always positively charged control without the poly. The charge reversal allowed for systemically injected nanocarriers, and the anticancer protein was produced at therapeutic quantities in the tumour with just one injection. Acid-induced peptide structural modification has been shown to be an effective method for tumor-directed administration of antimicrobial peptides. This is because the nanocarrier stimulates electrostatic contact between the cell membranes. The "pHLIP" or "acid-induced peptide delivery peptide" is a peptide that may fold into a stiff helix in acidic circumstances (53). The peptide's haphazard form rendered it resistant to cell membranes as it circulated in the circulation, which decreased non-local internalisation and resulted in passive buildup in the tumours. Because pHLIP was folded by the acidic environment of the tumour cells, it was then carried into the membrane of the cancer cells without needing to be endocytosed. The researchers demonstrated that pHLIP was capable of transporting the PNA's payload into the cell's cytoplasm in-vivo with a high selectivity towards the tumour. The PNA was created to ingest the cancer-causing microRNA-15 found in cancer cells.

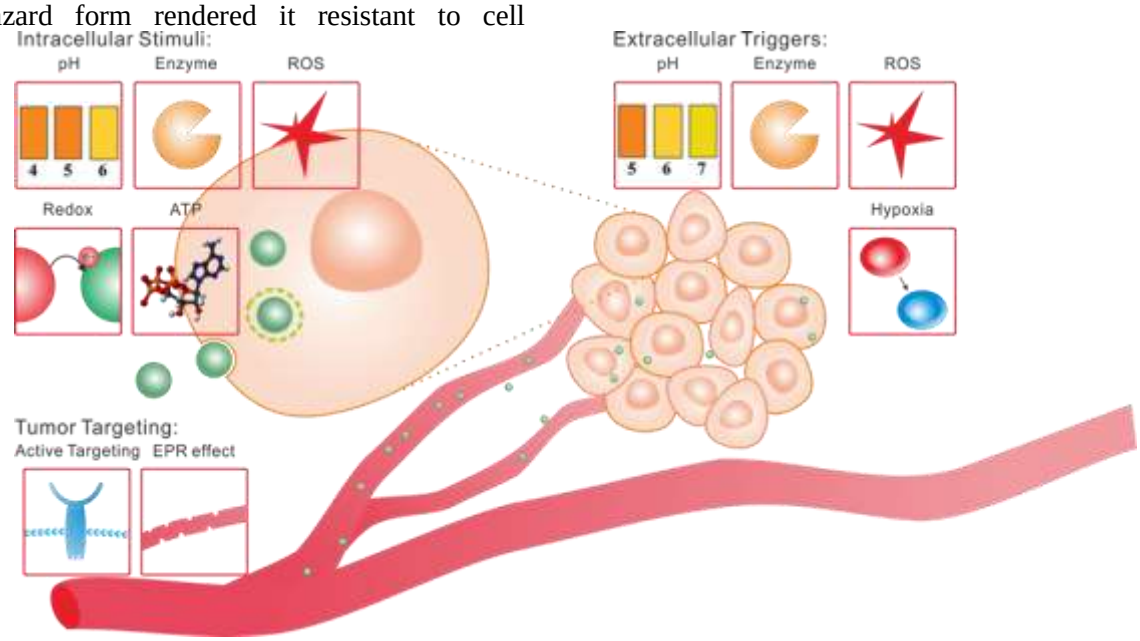

Figure 3: Intriguing Tumour Physiology for Precision Drug Delivery

Depending on the extracellular environment, the nano-carrier can enter the tumour by attaching to receptors that are particular to it or by inactivating through the EPR effect. Drug release that targets extracellular targets may be induced by physiological signals such pH gradients, enzymes, reactive oxygen species (ROS), and hypoxic settings. Alternatively, the nano-carrier may be activated to further enter the intracellular compartment. In addition to acids, enzymes, and reactive oxygen species, the extracellular environment can also function as a starting point for the intracellular transport of nanoparticles or medication release.

The high acidity of the vesicles in the intracellular environment is frequently used to activate intracellular transport or dissolve the nanoconstituted drug carriers for drug release, in addition to increasing extracellular acidity, which promotes cell absorption. Using a target ligand that may be lost intracellularly, a nano formulation with the goal of breaking the BBB may be used (54). The protein transferrin is transformed into 80-nm gold nano-carriers to act as the specific ligand, which starts the transcytosis process. Using an acid-degraded linker, the BBB is cross-referenced via receptor-mediated transcytosis. The gold nano-harriers first attach to the transferrin receptors on the blood side of the transcytosis pathway, then when the vesicles get acidic, the acid-labile linker disintegrates and releases the gold nano-harriers to the brain side. The transcytose efficacies of formulations with the acid cleavageable linker were much greater than those of formulations with non-cleavageable formulas. For efficient and acid-cleavable siRNA administration, acyclamide-dextrans was created (55), The SiRNA cargo is swiftly liberated when the transformed polysaccharide is degraded by endosomal acids due to an acetal linker that binds them collectively. For another sort of acidity trigger trafficking in the intracellular, a DNA-based nano-carrier was developed that can shed the modified targeting ligands after they have

been internalised in endosomes and disclose the membrane disruptor molecules for endosomal escape (56). The subject of considerable study has been acidity-induced intracellular trafficking as opposed to endolyosomal acidity-induced drug release. A recent demonstration of a novel method for mediating acid-induced drug release and removing metallic nano-carriers from the body by using liquid metal's acid response shows that this method is more efficient than traditional nano-carrier degradation by disintegrating labile linkers (57). In this system, a low viscosity alloy of eutectic metals (gallium, indium) is used to produce nanocarriers at ambient temperature. In order to load the medicine, thiolated b-cyclodextrine is used to stabilise the liquid metal after it has been sonicated into a nanocarrier and targeted to the cancer. The changed ligand modified liquid metal nano-carrier may target the cancer cells after systemic injection and penetrate the cancer cells through macropinocytes. The altered ligands and the drug they carried are subsequently ejected from the liquid metal as a result of endosomal acidicity. The histology investigation showed that the drug produced by the model drug, DOX, diffused into the cancer cells' nucleus, causing a significant remission. Compared to mercury, DOX is a far more biocompatible liquid metal. Over a three-month period, platelets and organs (such as the liver and kidney) in animal models examined for toxicological effects on the empty nano-carriers exhibited no discernible harm. Additionally, the liquid metal's corrosive byproduct reduced the cancer cells' medication resistance.

4.2 Enzyme activity

The development of pathological diseases such as inflammation or cancer is typically accompanied by an increase in the production of specific hydrolysis enzymes (e.g. protein, phosphate, or glycosporease) compared to normal conditions (58). Cancer cells tend to be more aggressive when enzymes like MMP (Matrix-Metalloproteinase) and phospholipase (Phospholipase-Hyaluronidase) and gelatine (Gelatinase) are released into the tumour's extracellular matrix. These enzymes can either activate cellular internalisation molecules or trigger drug release directly from the cell, which is two of the most popular triggers for drug delivery to the tumor. Just like cancer cells, they also have special internal enzymes like furin, kinases, esterases and cathepsins (59) were also shown as potential triggers. As the enzyme specific sensor and actuators, substrates that could be precisely cleaved by these enzymes were inserted into the nanocarriers.

MMP is by far the most common target for nano-carriers that utilise extracellular pathways to activate or release peptides. A model peptide that is activated by MMP is a peptide that is capable of penetrating the cell membrane. This peptide is produced by the synthesis of polyargininin (a peptide that is positively charged and facilitates strong cell internalisation) and a polyanion which neutralises the positive charges through the cleavage of an MMP 2/9 cleavage linker. This polyanion moiety acts as a barrier to the electrostatic interaction between polyargininine and cell membrane. This reduces cellular absorption in circulation until it is broken off by the peptide MMP- 2/9. The MMP activating peptide has been shown to increase tumor specific accumulation of imaging agent by 3-fold in in-vivo experiments. This peptide has also been shown to be altered by MMP drug delivery nano-carriers for anticancer drugs (60). This method was modified with a peptide, and the increased number of nano-carriers allowed for the simultaneous delivery of two separate anticancer medications - a plasmid encoding siRNA (for angiogenesis suppression) and a small molecule agent that kills cancer cells. When compared to nano-carriers coated with non-responsive peptides, MMP-2 led the nanoparticle to be internalised, making it more sensitive to tumor-targeted genes and chemotherapies. This resulted in a significant decrease in blood vessel development and increased cancer cell death in a mouse model of glioma. The MMP-2 also triggered a micelle that shed PEG, which was utilised to deliver paclitaxel, a hydrophobic medication. A cleavage peptide of MMP-2 was coupled with a hydrophobic peptide and a hydrophilic peptide to generate the amphiphilic component of the micelle's building block, PEG2000-peptide-PTX. To create TAT1000-PE, a TAT peptide was coupled to a shorter PEG peptide chain and a hydrophobic component (phosphoethanolamine) in the cancer microenvironment. The peptide was broken to disclose the hidden TAT peptide for better cellular absorption. In addition to regulated cellular internalisation, an MMP-degradable peptide is being investigated as a paradigm for controlled drug release in nanocarriers (61). Other tumor-associated enzymes, in addition to MMP, were investigated for regulated anticancer medication delivery. Furin is an essential secretase convertase that is found both on the cell membrane and in the intracellular compartment

(mostly the Golgi network) (62). Furin peptide serves as the substrate, and it is integrated into the graphene-based nano-carrier. Furin overproduction on the cancer cell membrane modulates medication release and nanoparticle internalisation (63). In this approach, TRAIL, a model cytokine, is conjugated with a furin susceptible peptide. TRAIL is then conjugated onto the GED sheet via a PEG (polyethylene glycol) linker. The DOX is loaded into the GED sheet by π-π stacking. When TRAIL is broken down in the cell membrane by the cell membrane related furin, the nanoparticle is released into the cancer microenvironment through the EPR effect. The remaining nano-carrier is internalised into the finalosomal compartment and delivers DOX. Furin cleavable nano-carrier demonstrated significantly more antitumour activity compared to non-degraded competitors. Sequential distribution that benefits extracellularly overexposed hyaluronidases (64). This method shapes the nanocarrier into a core-shell structure. The liposome serves as the DOX nanocarrier's loading core, while the HA gel serves as the loading shell. Hyaluronidases degrade the HA gel, allowing the TRAIL nanocarrier to enter the extracellular region and be easily internalised. We're also investigating novel enzymes linked to cancer development. Legumain, for example, is a protein that is overexpressed in tumor-related macrophages. After hypoxia/famine, it can be transported from the cytochrome P450 system to the membrane. The TAT side chain is conjugated to the AAN tripeptide, which connects the drug-containing liposomes to the changed peptide (65). The AAN alteration reduced 72.65% of TAT-induced cellular internalisation, which may be restored by removing the legumain.

4.3 Reducing gradient

The availability of additional reducing agents (NADPH, NADH, and THIODOXER) that sustain intracellular GSH concentrations in the range of 2-10 mM has drawn the attention of drug delivery specialists to the diminishing gradient between intracellular and extracellular space. Extracellular GSH levels, on the other hand, ranging from 2 to 20 M. Tumour GSH levels are at least four times greater than in normal tissues, boosting the selectivity of reduction gradient-based nanocarriers (66).

Nanocarriers are often linked to GSH-sensitive connections, especially in the form of disulfide bonds. These bonds are stable in the slightly oxidized extracellular space, but once they cross the plasma membrane, they either turn into thiols or undergo thiol-dissulfide exchange because of interactions with reducing agents. For example, disulfide bonds to control a "cyclodextrin-based capping" using folic acid in MSN nano-carriers. They also used disulfide bond connections between low-generation polyamide dendrimers and branched polyethylene glycoprotein shells (PAMAMs) to improve gene and chemical delivery. The dendrimer loaded with siRNA and a co-loaded dendrimer with DOX was exposed to passive drug release because of breakage of the disulfide bonds in the intracellular space (67). The nano-carrier was built utilizing the Particle Replication in Nonwetting Templates (PRINT) approach, which allows for SiRNA entrapment or conjugation. The probability of burst release was greatly minimised due to the covalent nature of SiRNA conjugation when compared to the Gel Entrapment-Based loading approach.

Selenium belongs to the same chemical family as sulphur, which means it contains more electrons than sulphur, making it a greater electron giver than acceptor. Using the diselenide link, we were able to polymerize a low molecular weight PEI into the nanosystem and electrostatically complex the DNA cargo. In addition, we were able to convert ferrocenium's cation, which is charged and hydrophilic during GSH reduction, into an amphiplastic building block for the fabrication of redox sensitive nanoassemblies (68). Pillararene is a hydrophobic building block that may be formed into amphiphalic conjugates by sandwiching it between ferrocenium and hydrophobic amphiphilic cations. Through electrostatic contact during sonication-mediated assembly, the amphiphilic amphiphile enhances effective cellular absorption and loading of SiRNA. Following cell internalisation, ferrocenium is reduced to ferrocene, which is then reduced back to ferrocenium. The polarity of the ferrocene is switched from amphiphalic to hyrophobic, which destabilises the assembly and allows the SiRNA to be released.

4.4 ROS

ROS such as singlet oxygen ($1O_2$), anion radicals (O_{2-}.), hydroxyl radicals (.OH), and hydrogen peroxide (H_2O_2) are formed during the intracellular metabolism of oxygen. Damaged ROS scavengers (such as antioxidant enzymes) and aggressive metabolism result in hazardous ROS accumulation inside cancer cells (69). ROS levels in tumour cells may be 10 to 100-fold higher than in normal cells, which adds to DNA damage or mutation, increasing tumour aggressiveness. ROS buildup is a characteristic

shared by many disorders, including inflammation, neurodegenerative disease, diabetes, and cardiovascular disease (70). Nanocarriers were created by incorporating labile bonds that could either be cleaved (such as thiolketal, aryl boronic acid, or proline) or undergo polarity shift (such as thiolester, propylene sulphide, or ferrocene) upon oxidation in order to harness the ROS as a physiological cue for regulated drug delivery.

For siRNA oral delivery, a thioketal-based polymer called poly-(1,4-phenyleneacetone dimethylene thioketal) was utilised. The polymer is resistant to acid, alkaline, and proteolytic degradation, but it is vulnerable to ROX-mediated cleavage, allowing for site-specific delivery of nanopariticle to ROS-producing inflamed or cancerous intestines. Based on ROS-triggered protein deprotection, we developed a method for spatial-temporal modulation of protein function after delivery (71). A 4-nitrophenyl-4-(4,4,5,5-tetramethyl-1,3,2-dioxaborolan-2-yl) benzyl carbonate caged the key lysine residue of the model anticancer protein RNase A through a ROS labile boronic acid linker. Only the aryl boronic acid connected cage could be cleaved off after H_2O_2, whereas a non-degradable control failed to activate RNase A. The ROS labile boronic acid liker has also been incorporated into an activatable CPP for in-vivo agent administration (72). The positively charged CCP (Arg9), like the MMP activatable CPP, was caged by an anionic moiety (Glu9) via the ROS sensitive 4-boronic mandelic acid linker. When exposed to H_2O_2, the peptide fractured, promoting intracellular penetration.

ROS-driven polymer polarity flipping was used to create a polymeric shell that controls nanocrystal aggregation. By altering the affinity between the thioester-based amphiphilic polymer and the hydrophobic PTX nanocrystals, non-oxidative core-shell nanocarriers were created. By converting hydrophobic thiolesters to hydrophilic sulfoxide or sulfone, ROS weakens the shell to enable PTX release. The release of medicine during oxidation is controlled by the polarity shift of ferrocenium and ferrocene (73). A polymer nanocapsule with a liquid core containing ferrocenium and a medication has been produced. The drug was released from the nanocapsule when the local polarity of the polymer was altered by oxidation.

4.5 Hypoxic condition

Because the tumour vasculature is disrupted, oxygen supply is limited to more than 200m distant from the heart's capillaries. As a result, hypoxia is a prevalent characteristic of primary tumours. The hypoxic environment provides pressure on cancer cell variations to survive, resulting in more chemocompromise, death-competent, invasive, and metastatic cancer cells. Hypoxia is a significant target for cancer therapy because it promotes tumour development and treatment resistance. Much effort has been expended in order to target the hypoxic zone. Hypoxia-promoting chemotherapeutics, for example, have been created, and anaerobic bacteria have been engineered to generate tumor-suppressing protein. Because tumours exhibit severe hypoxia but normal tissues do not, hypoxia has been utilised to construct tumor-targeted nanocarriers for theranostics (74).

To operate as a trigger, hypoxia-labile connections were frequently introduced to nanoparticles. Azobenzene was employed as a hypoxia-cleavable linker in the construction of a PEG-sheathed nanocarrier capable of delivering hypoxia-specific siRNA. The nanocarrier was constructed using a PEG, Azobenzene, PPEI, and lipid DOPE building block. The SiRNA payload was electrostatically complexed before being introduced into the nano-carrier. As the PEG shell cracks, the siRNA-loaded micelle diffuses to a hypoxic tumour location, exposing the cationously-charged PEI layer for cancer cell absorption. Two hypoxia-sensitive nitrogen molecules (NI) were added to the side chain of a hydrophilic polymer named Carboxymethyl Dextran (75). Due to the hydrophobic nature of NI, the amphiphilic polymer may self-assemble into nanocarriers containing a hydrophobic medicament. When the nanocarrier was exposed to a hydrophobic environment, the NI group deteriorated to a hydrophilic derivative, destabilising the self-assembly for drug release. Both in-vitro and in-vivo, the hypoxia-responsive nanoparticle demonstrated hypoxic cancer cell/tumor selectivity. Despite progress in exploiting hypoxia to initiate nanocarrier activation or drug release, it may be challenging to deliver nanocarriers to cancer sites remote from blood arteries.

4.6 ATP gradient

During cancer formation, several different kinds of metabolites are elevated. The "molecular unit of currency" in metabolic energy transmission is ATP. The concentration of ATP varies dramatically between outside (5 M) and inside (1 - 10 mM) settings. Cancerous tissues have higher levels of intracellular ATP (76). As a result, ATP

has emerged as a novel physiological trigger that has lately been studied for regulated intracellular drug delivery.

The most widely used ATP sensitive moiety in the creation of ATP-responsive nanosystems is the ATP binding aptamer (a short single stranded DNA). During DOX delivery, the ATP aptamer functions as both an ATP sensor and a drug release actuator. In this formulation, the ATP aptamer and its complementary strand were hybridised into a DNA duplex, resulting in a "GC" pair for loading the DOX. Before being coated with a HA polymer shell, the DOX-loaded DNA duplex was compressed using a positively charged peptide protamine. The systemic dispersion of the nanoparticle allowed it to collect in cancer tissue, where the HA shell was broken by the tumor's HAase-rich environment and the DOX-loaded DNA duplex was shuttled intracellularly. When exposed to the intracellular compartment's high ATP level, ATP competitively binds the ATP aptamer and dissociates the DNA duplex for DOX release. When compared to a nonresponsive DNA core, the ATP aptamer-based nanocarrier dramatically reduced tumour development. The ATP aptamer's short length makes it simple to adapt to many types of nanosystems (77).

Aside from the typical ATP aptamer, many ATP binding chemicals were investigated for application in the development of ATP-responsive DDSs. The significant affinity between ATP and Zn^{2+}-dipicolylamine was used to create an ATP-responsive theranostic system (78).

5.Research Objectives

The creation of a DNA-based nanostructure that could serve as a platform for the delivery of different medicines is the aim of this dissertation. The design principles for targeted nanomedicine will be introduced first, and then there will be a discussion of physiological challenges and strategies for overcoming them. A summary of recent developments in the field of DNA nanostructure based nanomedicine will then be given, with a specific focus on the use of DNA as a nanomaterial for therapeutic delivery. The dissertation's main body will show how rolling circle amplification has been used to create various medication delivery methods. A chemotherapeutic anticancer drug, a ribonucleoprotein complex for altering genomic sequence, and a cytokine that triggers apoptotic signalling in cancer cells were all delivered by the DNA nanoclew.

6. MATERIAL AND METHODS

6.1 Chemicals, Reagents and Instruments

6.1.1 Chemicals and Reagents

Unless otherwise noted, all chemicals and reagents were of AR Grade, obtained from a local Sigma-Aldrich source and utilized exactly as received. Cadila Pharmaceuticals Ltd. (Oncocare), Ahmedabad, India, provided 5-FU as a gift sample. The DNA oligos were supplied by Eurofins Genomics India Pvt Ltd, Banglore, India. Deoxyribonuclease I from the bovine pancreas, CircLigase II ssDNA Ligase, DNA ladder, dNTP, Folic acid-polyethylene glycol 2000-N-hydroxysuccinimidyl ester (FA-PEG-NHS) and Exonuclease I were purchased from Sigma-Aldrich Chemicals Private Limited as lyophilized powder. Bst 2.0 DNA polymerase was purchased from Livgen Biotechnologies, Bengaluru, Karnataka, India. A bright, green-fluorescent dye, Alexa Fluor® 488 NHS Ester (or hydroxysuccinimidyl ester) was procured from Thermo Fisher Scientific Inc. Glycerol dimethacrylate was purchased from N Shashikant & Co., Mumbai, India. GelRed Nuclic acid Gel Stain was purchased from Biological Scientific Solutions, New Delhi, India. Mono-sulfo-N-hydroxysuccinimido Au-nanoparticles was purchased from Indian Platinum Pvt. Ltd, Mumbai, India. Thermo Scientific's Pierce BCA Protein Assay Kit is a detergent-compatible bicinchoninic acid (BCA)-based formulation for the colorimetric detection and quantification of total protein was procured from Thermo Fisher Scientific Inc.

6.1.2 Instruments

The melting points of the compounds were determined in open capillaries using Thermonik Precision Melting point cum Boiling point apparatus (C-PMB-2, Mumbai, India). The melting points reported here in are in the Celsius scale and are uncorrected. Precoated silica gel-G plate activated at 110o C for 30 min. used for thin layer chromatography and the spots developed in iodine chamber. Though different solvent systems were employed, Rf values are reported for better comparable solvent systems, which are mentioned in the preceding text. The ultraviolet spectra measured in acetate buffer solution (pH = 4.3) (HPLC grade) on Shimadzu 1601 Spectrophotometer. IR spectra of compounds recorded using KBr pellets on FTIR-8400s, Shimadzu Kyoto, Japan, at Sharad Pawar College of Pharmacy, Wanadongri, Hingna Road, Nagpur. Zeta potential and particle size distribution recorded using a Zetasizer (Nano ZS, Malvern), at

CSIR - Central Mechanical Engineering Research Institute, Durgapur, W.B. The far-UV circular dichroism (CD) spectra were measured using a JASCO J-815 Circular Dichroism Spectrometer. Transmission Electron Microscopy (TEM) imaging were investigated using a 100 kV TEM (JEM-2000FX, Hitachi). Confocal laser scanning microscopy was performed using LSM 710, Zeiss.

7. Preformulation Studies

The initial quantitative evaluation of a drug's chemical stability and stability in the presence of additional excipients typically comes from preformulation experiments. The main goals of this inquiry are to find stable storage conditions for drugs in the solid state and to find excipients that work well with a formulation. The medication underwent preformulation tests, including IR spectroscopy identification, melting point assessment, solubility, maximum absorption spectra (λ_{max}), and partition coefficient research.

7.1 Identification (IR spectroscopy)

Infrared spectroscopy is a flexible technique for identifying and detecting pharmaceuticals as well as functional groups inside molecules. It records the infrared energy absorbed. Infrared spectroscopy can be used to evaluate pharmaceutical samples that are solid, liquid, or gaseous. FTIR equipment was used to scan the pure 5-fluorouracil over a range of 400-4500 cm^{-1} while mixing it with IR grade KBr.

7.2 Boiling point

The boiling point of open capillary tubes with one end, when an inverted capillary is inserted in the desired liquid and heated, was measured using a Thermonik Precision melting point equipment (C-PMP-2, Mumbai, India).

7.3 Solubility

The solubility of 1 mg of the medication 5-fluorouracil in 0.1 N NAOH, water, methanol, and ethanol was examined. Using ultrasonography, ethanol, and methanol, it was discovered that the medication was soluble in water.

7.4 Partition coefficient

When making a controlled release medicine using supercritical fluid technology, one significant consideration is the drug's solubility in supercritical carbon dioxide ($ScCO_2$).

The partition coefficient values of 5-FU was determined, into a separating funnel containing n-octanol solution (10 mL) was added an equal volume of saturated drug solution in water. The system was kept at room temperature for 24 h with intermittent shaking. Finally, aqueous and organic layers were separated, clarified by centrifugation at 1000 rpm for 5 min, and assayed by UV-Visible Spectoscopy.

7.5 Preparation of calibration curve of drug using UV spectrophotomter method

7.5.1 Preparation of Standard Stock Solution and Selection of Wavelength for Analysis

Accurately weighed 10 mg of 5-Fluorouracil was transferred to 40 mL volumetric flask separately, dissolved in distilled water by sonicater, sonicate up to 10 minute. The volume was adjusted with the same up to the mark to give final strength i.e. 100 μg/mL.

By appropriate dilutions with distilled water were prepared for each drug from the standard stock solution and scanned in the spectrum mode from 400 nm to 200 nm and their spectra were over laid.

i. Linearity

Calibration curve constructed was linear over the selected range of 2-12 μg/mL for 5-Fluorouracil at λ_{max} of 266nm. Each concentration was repeated three times. The assays were performed according to experimental conditions and the linearity of the calibration graphs were validated by the high value of the correlation coefficient and the intercept value.

8.Preparation and characterization of DNA nanoclews (NCl) by rolling circle amplification method

The DNA nanoclews (DNANCl) were created using rolling circle amplification (RCA). According to the manufacturer's instructions, a 5'-phosphorylated ssDNA template having DNA sequences as depicted in Table 4.1, was cyclized into a circular ssDNA template using CircLigase II ssDNA ligase, by following the below mentioned procedure as presented in Figure 4.1.

Table 1: Sequences of DNA Oligos

	Sequences (5'-3')
	Phospate-
Template (flexible arm, palindromic	GTTAATATTATTCGACGGGCCTGCTCGAGC
sequence FA-oligo hybridization site)	TCGAGCTTGCATCGTGCAGCCGAAGCTTG
	CACGCGTGCTATTAAT
Primer	GCACGCGTGCAAGC
cDNA oligo	GCTTGCACGCGTGC-NH_2

Figure 4. Synthesis of NCl by Rolling Circle Amplification

II A DNA oligo was utilised as the primer, and cyclized single-stranded DNA functioned as the template to create long chains of single-stranded DNA.

III Through intramolecular hybridization, the synthesised RCA product self-assembled into a nanoclew-like structure.

8.1Procedure for preparation of DNA Nanoclews by RCA method

Reaction mixture was prepaered which composed of 2.5 mM Manganese(II) chloride, 1 mM Trimethylglycin (betaine), and 5 U/µL CircLigase II ssDNA ligase; a thermostable enzyme that catalyses intramolecular ligation (i.e. circularisation) of ssDNA. To the 20 µL reaction mixture, 10 pmol ssDNA template was added to prepare cyclized templates. The cyclized template prepared in aforementioned step was incubated at 60°C for 1 hour before being treated with exonuclease I (1 U/µL) at 37°C for 45 minutes, followed by heat inactivation at 80°C for 15 minutes. The resulting cyclized ssDNA template was hybridised with 0.5 mM primer in an isothermal amplification buffer containing 0.2 mM deoxynucleoside triphosphates (dNTPs), the substrates for DNA polymerizing enzymes, at 95°C for 5 min. An isothermal amplification buffer composed of 20 mM Trizma Hydrochloride (Tris-HCl) pH 8.8, 10 mM Ammonium sulphate, 50 mM Potassim chloride, 2 mM Magnesium sulphate in 0.1% Tween 20. Bst 2.0 DNA polymerase in a concentration of 0.2 U/µL was added to the template-primer hybridized solution after it had been cooled to room temperature. The rolling circle amplification was then carried out at 60°C for 17 hours, followed by heat inactivation at 80°C for 20 minutes. The resulting NCl was dialyzed for 48 hours in a dialysis unit (20 K MWCO) (Slide-A-Lyzer, Thermo Scientific) against TE buffer (10 mM Tris pH 8.0, 1 mM EDTA).

8.1.1Estimation of particle size and surface morphology of NCl

A Zetasizer was used to measure the zeta potential and particle size distribution at 25°C unless otherwise noted. A high performance two angle particle, zeta-potential, and molecular size analyzer for better detecting aggregates and minute particles is the Zetasizer Nano ZS. Samples can be examined using dynamic light scattering and "NIBS" optics at extremely low or high concentrations. According to the dynamic light scattering hypothesis, small particles disperse more quickly than bigger ones due to their continuous random thermal motion, or Brownian motion. The study was carried out at CSIR - Central Mechanical Engineering Research Institute, Durgapur, West Bengal. Agarose gel electrophoresis was used to determine the sizes of the template and product using 0.8% (w/v)

agarose gel. The agarose gel was photographed under UV light after GelRed staining. Thermo Scientific's Nanodrop 2000C spectrometer was used to detect the DNA concentration in NCl. The observations of the peak of intensity, which corresponds to the majority of the mass in the system, are averaged over five measurements.

8.1.2Determination of percent yield and encapsulation efficiency

A previously reported approach was used to determine the encapsulation efficiencies of the various formulations. The RCA product's stability was examined by incubating it at 37°C for 48 hours in Dulbecco's Modified Eagle Medium (DMEM) media with 10% foetal bovine serum (FBS). NCl was put onto a silicon wafer (Ted Pella), dried, and then analysed using Nanoscope (Veeco, Santa Barbara, CA) in tapping mode in ambient air for atomic force microscopy, a form of scanning probe microscopy.

To evaluate the efficacy of encapsulation, 1 mg of NCl were lysed in 10 µL of dimethyl sulfoxide (DMSO) and then diluted in 90 µL of PBS. The amounts of Cas9 protein and DNA were determined using commercial kits (ThermoFisher Scientific) and the widely used bicinchoninic acid (BCA) test and Pico-Green assay, respectively. NCl without encapsulants was employed as a baseline. NCl (3-5 mg) were suspended in 1 mL PBS (pH 7.4) and incubated at 37 °C with gentle shaking to define drug release. The NCl suspension was centrifuged for 15 minutes at a speed of 15000 rpm during each sampling time. To quantify the Cas9 protein or DNA, the supernatant was collected and reconstituted with an equivalent volume of PBS for continuous release monitoring. The Cas9 protein or DNA was discovered using the same BCA and Pico-Green techniques.

9. Preparation and characterization of DNase I nanocapsule (NCa)

9.1 Preparation of DNase I nanocapsule

DNase I was cross-linked using a pH sensitive cross-linker after being encapsulated in a single protein naoncapsule. DNase I lyophilized powder was dissolved to 1 mg/mL in 5 mM bicarbonate buffer (pH 8.3) with a PDI of 0.38 0.03 using Zetasizer (Nano ZS, Malvern). DNase I solution 1 mL was combined with 200 mg/mL acrylamide (AAm) at 4°C. The positively charged monomer N-(3-aminopropyl) methacryl amide (APMAAm) was introduced after 10 minutes of churning. To commence polymerization, the pH responsive cross-linker glycerol dimethacrylate (GDA) was introduced, along with 25 µL ammonium persulfate (100 mg/mL in deoxygenated and deionized water) and 3 µL N,N,N',N'-tetramethyl ethylene diamine. The molar ratio of AAm/APMAAm/GDA was 10/1/0.14. After 60 minutes, the buffer was changed to phosphate-buffered saline (pH 7.4) in an ultracentrifuge unit (MWCO 30 KDa, Millipore) to remove excess monomers and initiators.

9.2 Characterization of DNase I Nanocapsule

Thermo Scientific's Pierce BCA Protein Assay Kit used for the colorimetric detection and quantification of total protein. The biuret reaction combines the well-known protein reduction of Cu^{+2} to Cu^{+1} in an alkaline medium with a novel BCA-containing reagent for highly sensitive and specific colorimetric detection of the cuprous cation (Cu^{+1}). The purple reaction result of this assay is caused by the chelation of two BCA molecules with one cuprous ion. This water-soluble substance displays a substantial 562 nm absorbance that increases approximately linearly with protein content (20-2000 µg/mL). The BCA approach is not a real end-point method because the final color is still changing. On the other hand, during incubation, the rate of continuous color development is moderate enough to allow for the analysis of several samples at once. The protein content of NCa was determined using the BCA colorimetric protein assay with bovine serum albumin (BSA) as the reference. The macromolecular structure of the protein, the number of peptide bonds, and the presence of four specific amino acids (cysteine, cystine, tryptophan, and tyrosine) are thought to be responsible for colour formation with BCA. The far-UV circular dichroism (CD) spectra of natural DNase I and NCa were measured at 20°C in 0.1 M phosphate buffer (pH 7.4) with a protein content of 0.2 mg/mL.

9.2.1 Estimation of particle size and surface morphology of DNase I nanocapsules

The size and zeta potential of native DNase I and NCa were determined using dynamic light scattering. Methylenebisacrylamide (MBA), a non-degradable cross-linker, was used instead of GDA for the non-degradable NCa, but all other parameters remained constant. The morphology of NCa was investigated by TEM. For Transmission Electron Microscopy (TEM)

imaging, the samples were dropped on a TEM copper grid (300 mesh) (Ted Pella) and stained with 2% (w/v) uranyl acetate (dissolved in 50% ethanol). DNase I activity was measured at 37 °C in 200 mM phosphate buffer containing 2.5 mM $MgCl_2$ and 0.5 mM $CaCl_2$, with salmon DNA sodium salt (0.2 mg/mL) as the substrate. The Nanodrop 200ºC from Thermo Scientific was used to track A260 fluctuations over time.

10. Assembly and characterization of NCl/NCa

Size and zeta potential of NCl/NCa was measured by a Zetasizer. To visualize the assembly by confocal laser scanning microscope (CLSM), DNase I was conjugated with Alexa Fluor® 488 N-hydroxysuccinimidyl ester (AF488-NHS) to obtained AF488 decorated DNase I (AF488-DNase I). NCl 10 µg/mL was mixed with NCa 40 µg/mL before each use. 1 mg of DNase I was combined with one millilitre of 0.1 M bicarbonate buffer (pH 8.3), and the DNase I solution was then stirred while an equimolar quantity of AF488-NHS (dissolved in anhydrous DMSO) was added. The excess AF488-NHS was removed by ultracentrifugation after the reaction had been maintained at room temperature for one hour. AF488-NCa was created by encapsulating AF488-DNase-I in an acid degradable protein capsule, as previously described. CLSM enables the 3D localisation of tagged target molecules in cells. The LSM 710's quick and flexible detection technology, paired with the high performing In Tune (488 to 640 nm, >1.5 mW per wavelength), allows the fluorescence signal to be detected extremely close to the excitation wavelength. Furthermore, In Tune is the ideal adaptable laser system for detecting previously unmeasured fluorescence lifetimes of dyes. NCl was visualized by thefluorescence of the loaded 5-FU. The 5-FU/NCl/AF488-NCa was immobilized in 1% agarose gel and observed with CLSM (LSM 710, Zeiss). Gold nanoparticles (AuNPs) are excellent scaffolds for the development of biosensors for a variety of targets. The visible plasmon resonance of AuNPs can be exploited by dark-field imaging to identify particle structures. This efficient method has been extended to detect targets like DNA, mRNA, and proteins due to AuNPs' notable local field increase. In typical LSPR investigations, the amount of wavelength shift is directly proportional to analyte concentration, therefore a lower concentration of analyte induces less LSPR shift. Because clinical concentrations of analytes are typically too low for this approach to detect, these tests are not appropriate for early illness detection. In order to observe NCl/NCa by TEM, AuNP was coupled onto DNase I for imaging. In PBS buffer (pH 7.4), mono-sulfo-N-hydroxy-succinimido AuNP was reacted with native DNase-I at a molar ratio of 4:1 for 1 hour. To remove extra AuNP, gel filtering with a size exclusion chromatography gel column, Superdex-75, was utilised. The Superdex®75 10/300 GL gel filtration column is prepacked and suited for high-resolution, semipreparative, and analytical biomolecule separations. Superdex® 75 can separate molecules ranging in molecular weight from 3000 to 70000. AuNP and DNase-I concentrations were determined using UV-Visible spectra and molar extinction coefficients (AuNP, 155000 $M^{-1}cm^{-1}$ at 420 nm, DNase I, 36750 $M^{-1}cm^{-1}$ at 280 nm). The resulting Au-DNase-I had a molar ratio of 0.91 AuNP/DNase-I and was encapsulated in the nanocapsule (Au-NCa) using the same method as native DNase-I. The Au-NCa was mixed with NCl before being placed on a TEM grid and washed with deionized water. Silver enhancement was employed to improve TEM imaging by floating the grid in fresh silver enhancement reagent (Nanoprobe) for one minute. The grid was then cleaned with deionized water and dyed with 1% sodium phosphotungstate at pH 7.0. This method yields homogenous 3-4 nm silver-coated AuNP. After incubating NCl/NCa samples for 2 hrs in phosphate buffer at pH 7.4 and pH 5.4, AFM was used to examine PH-induced NCl/NCa disintegration.

11. Loading of Drug (5-Flurouracil) and release

NCl's ability to quench 5-FU fluorescence was used to determine its capacity to load 5-FU. At varied final concentrations (0.15-2.4 g/mL), the fluorescence of 5-FU/NCl was evaluated using a microplate reader (Infinite M200 PRO, Tecan) (excitation 480 nm, emission 520-800 nm). To evaluate the 5-FU loading efficiency, 10 µg/mL NCl was incubated for 1 hour at room temperature with various dosages of 5-FU (5-160 µM, 5-FU /NCl mass ratio of 0.3-9.3). After centrifugation at 14000x for 10 minutes, the 5-FU concentration in the supernatant was determined by detecting 5-FU fluorescence (excitation 450 nm, emission 360 nm).

12. Surface Morphology and Particle Size Estimation of a Drug-loaded NCl/NCa

congugate

The mass of 5-FU trapped divided by the dosage of 5-FU is used to determine 5-FU entrapment efficiency. The ratio of the initial 5-FU addition to the 5-FU in the centrifuged supernatant is used to calculate the amount of 5-FU that has been trapped. To determine a DNA carrier's 5-FU loading capacity, use the mass of 5-FU entrapped/(mass of 5-FU entrapped + mass of carrier) formula. 5-FU fluorescence recovery was measured after incubating 5-FU/NCl/NCa or 5-FU/NCl/cNCa for 260 minutes at 37°C in 0.2 M phosphate buffer (pH 7.4, 5.4) containing 2.5 mM MgCl2 and 0.5 mM $CaCl_2$. 5-FU fluorescence was seen after collecting samples and centrifuging them at 14000 x g for 10 minutes.

13. Conjugation of NCl with Hyaluronic acid

It is good in attracting and holding onto water. Hyaluronic acid (HA) is a polymer or long chain of carbohydrates. When there is a lot of blood flow, pancreatic cancer can become hyperdense, causing the veins to collapse and the tumours to become extremely hard. The 3' end of the complementary DNA (cDNA) oligo was altered with NH2 to facilitate HA conjugation (Table 4.1). After dissolving the oligo in 0.1 M bicarbonate buffer (pH 8.3), hyaluronic acid-PEG 2000-N-hydroxy succinimidyl ester (HA-PEG-NHS) was added and mixed in. The reaction was kept at ambient temperature for the entire night while being shielded from light. The conjugation product (cDNA-PEG-FA) was dialyzed in a dialysis device for 48 hours against deionized water. cDNA-PEG-HA was produced, and it was hybridized with NCl at 95 °C for 5 minutes before being cooled to room temperature. The repeating unit in NCl has a 100:1 molar ratio to cDNA-PEG-FA. A Zetasizer was used to measure FA-NCl's size and zeta potential.

15. References:-

1. Fox CB, Kim J, Le LV, et al. Micro/nanofabricated platforms for oral drug delivery. J. Control. Release 2015; 219: 431-44.
2. Nair M, Jayant RD, Kaushik A, et al. Getting into the brain: Potential of nanotechnology in the management of NeuroAIDS. Adv Drug Deliv Rev 2016; 103: 202-17.
3. Williams AC, Barry BW. Penetration enhancers. Adv. Drug Del. Rev. 2012; 64, Supplement: 128-37.
4. Farra R, Sheppard NF, McCabe L, et al. First-in-Human Testing of a Wirelessly Controlled Drug Delivery Microchip. Sci. Transl. Med. 2012; 4: 122ra21.
5. Wessely R. New drug-eluting stent concepts. Nat Rev Cardiol 2010; 7: 194-203.
6. Hu Q, Sun W, Wang C, et al. Recent advances of cocktail chemotherapy by combination drug delivery systems. Adv Drug Deliv Rev 2016; 98: 19-34.
7. Park J, Park J, Pei Y, et al. Pharmacokinetics and biodistribution of recently- developed siRNA nanomedicines. Adv Drug Deliv Rev 2015; 104: 93-109
8. Langer R. Drug delivery and targeting. Nature 1998; 392: 5-10.
9. Mukker JK, Singh RSP, Derendorf H. Pharmacokinetic and pharmacodynamic implications in inhalable antimicrobial therapy. Adv. Drug Del. Rev. 2015; 85: 57-64.
10. Ranquin A, Versées W, Meier W, et al. Therapeutic Nanoreactors: Combining Chemistry and Biology in a Novel Triblock Copolymer Drug Delivery System. Nano Lett. 2005; 5: 2220-4
11. Siepmann J, Peppas NA. Modeling of drug release from delivery systems based on hydroxypropyl methylcellulose (HPMC). Adv. Drug Del. Rev. 2012; 64, Supplement: 163- 74.
12. Valencia PM, Farokhzad OC, Karnik R, et al. Microfluidic technologies for accelerating the clinical translation of nanoparticles. Nat. Nanotechnol. 2012; 7: 623-9.
13. Park K. Facing the Truth about Nanotechnology in Drug Delivery. ACS Nano 2013; 7: 7442-7.
14. Peppas NA. Historical perspective on advanced drug delivery: How engineering design and mathematical modeling helped the field mature. Adv. Drug Del. Rev. 2013; 65: 5- 9.
15. Moroz E, Matoori S, Leroux J-C. Oral delivery of macromolecular drugs: Where we are after almost 100 years of attempts. Adv. Drug Del. Rev. 2016; 101: 108-21
16. Wiedersberg S, Guy RH. Transdermal drug delivery: 30 + years of war and still fighting! J. Control. Release 2014; 190: 150-6.
17. Uhrich KE, Cannizzaro SM, Langer RS, et al. Polymeric systems for controlled drug release. Chem. Rev. 1999; 99: 3181-98.
18. Park K. Controlled drug delivery systems: Past forward and future back. J. Control. Release 2014; 190: 3-8.
19. Santus G, Baker RW. Osmotic drug delivery: a review of the patent literature. J. Control. Release 1995; 35: 1-21.

20. Peppas NA, Hilt JZ, Khademhosseini A, et al. Hydrogels in Biology and Medicine: From Molecular Principles to Bionanotechnology. Adv. Mater. 2006; 18: 1345-60.
21. Farokhzad, O. & Langer, R., 2015 Farokhzad OC, Langer R. Impact of Nanotechnology on Drug Delivery. ACS Nano 2009; 3: 16-20.
22. Traverso G, Langer R. Engineering precision. Sci. Transl. Med. 2015; 7: 289ed6-ed6
23. Langer R, Weissleder R. Scientific discovery and the future of medicine. JAMA 2015; 313: 135-6.
24. Coombes RC. Drug testing in the patient: Toward personalized cancer treatment. Sci. Transl. Med. 2015; 7: 284ps10
25. Collins, F. & Varmus, H., 2015 Collins FS, Varmus H. A New Initiative on Precision Medicine. N. Engl. J. Med.2015; 372: 793-5.
26. Mirnezami R, Nicholson J, Darzi A. Preparing for Precision Medicine. N. Engl. J. Med. 2012; 366: 489-91.
27. Davis ME, Zuckerman JE, Choi CHJ, et al. Evidence of RNAi in humans from systemically administered siRNA via targeted nanoparticles. Nature 2010; 464: 1067-70.
28. Vogelstein B, Papadopoulos N, Velculescu VE, et al. Cancer Genome Landscapes.Science 2013; 339: 1546-58
29. Albanese A, Tang PS, Chan WCW. The Effect of Nanoparticle Size, Shape, and Surface Chemistry on Biological Systems. Annu. Rev. Biomed. Eng. 2012; 14: 1-16.
30. Tenzer S, Docter D, Rosfa S, et al. Nanoparticle Size Is a Critical Physicochemical Determinant of the Human Blood Plasma Corona: A Comprehensive Quantitative Proteomic Analysis. ACS Nano 2011; 5: 7155-67.
31. Peppiatt CM, Howarth C, Mobbs P, et al. Bidirectional control of CNS capillary diameter by pericytes. Nature 2006; 443: 700-4.
32. Hobbs SK, Monsky WL, Yuan F, et al. Regulation of transport pathways in tumor vessels: role of tumor type and microenvironment. Proc Natl Acad Sci U S A 1998; 95: 4607-12.
33. Chauhan VP, Jain RK. Strategies for advancing cancer nanomedicine. Nat. Mater.2013; 12: 958-62.
34. Sun W, Gu Z. ATP-Responsive Drug Delivery Systems. Expert Opin. Drug Del. 2016; 13: 311-4.
35. Sun W, Ji W, Hu Q, et al. Transformable DNA nanocarriers for plasma membrane targeted delivery of cytokine. Biomaterials 2016; 96: 1-10.
36. Yoo J-W, Mitragotri S. Polymer particles that switch shape in response to a stimulus. Proc. Natl. Acad. Sci. U. S. A. 2016; 107: 11205-10.
37. Harush-Frenkel O, Rozentur E, Benita S, et al. Surface charge of nanoparticles determines their endocytic and transcytotic pathway in polarized MDCK cells. Biomacromolecules 2008; 9: 435-43.
38. Han, S., et al., 2015 Han SS, Li ZY, Zhu JY, et al. Dual-pH Sensitive Charge-Reversal Polypeptide Micelles for Tumor-Triggered Targeting Uptake and Nuclear Drug Delivery. Small 2015; 11: 2543-54.
39. Huang S, Shao K, Liu Y, et al. Tumor-Targeting and Microenvironment-Responsive Smart Nanoparticles for Combination Therapy of Antiangiogenesis and Apoptosis. ACS Nano 2013; 7: 2860-71.
40. Harush-Frenkel O, Rozentur E, Benita S, et al. Surface charge of nanoparticles determines their endocytic and transcytotic pathway in polarized MDCK cells. Biomacromolecules 2008; 9: 435-43.
41. Hu Q, Sun W, Wang C, et al. Recent advances of cocktail chemotherapy by combination drug delivery systems. Adv Drug Deliv Rev 2016; 98: 19-34.
42. Demoulin JB, Essaghir A. PDGF receptor signaling networks in normal and cancer cells. Cytokine Growth F. R. 2014; 25: 273-83.
43. Cui J, Bjornmalm M, Liang K, et al. Super-soft hydrogel particles with tunable elasticity in a microfluidic blood capillary model. Advanced materials (Deerfield Beach, Fla.) 2014; 26: 7295-9.
44. Wong PT, Choi SK. Mechanisms of Drug Release in Nanotherapeutic Delivery Systems. Chem. Rev. 2015; 115: 3388-432
45. Chou LYT, Zagorovsky K, Chan WCW. DNA assembly of nanoparticle superstructures for controlled biological delivery and elimination. Nat. Nanotechnol. 2014; 9: 148-55
46. Chow, E. K.-H.; Ho, D. Sci. Transl. Med, Cancer nanomedicine: from drug delivery to imaging.2013, 5, No. 216rv214
47. Drmanac R., Sparks A. B., Callow M. J., Halpern A. L., Burns N. L., et al., Human genome sequencing using unchained base reads on self assembling DNA nanoarrays.

Science 2010, 327, 78-81.
48. Schuller, V. J.; Heidegger, S.; Sandholzer, N.; Nickels, P. C.; Suhartha, N. A.; Endres, S.; Bourquin, C.; Liedl, T. ACS Nano 2011, 5, 9696−9702
49. Li, J.; Pei, H.; Zhu, B.; Liang, L.; Wei, M.; He, Y.; Chen, N.; Li, D.; Huang, Q.; Fan, C. ACS A DNA nanostructure platform directed assembly of synthetic vaccines Nano 2011, 5, 8783−8789
50. Fleige E, Quadir MA, Haag R. Stimuli-responsive polymeric nanocarriers for the controlled transport of active compounds: Concepts and applications. Adv. Drug Del. Rev. 2012; 64: 866-84
51. Pang X, Jiang Y, Xiao Q, et al. pH-responsive polymer–drug conjugates: Design and progress. J. Control. Release 2016; 222: 116-29
52. Poon Z, Chang D, Zhao X, et al. Layer-by-Layer Nanoparticles with a pH-Sheddable Layer for in-vivo Targeting of Tumor Hypoxia. ACS Nano 2011; 5: 4284-92.
53. Tseng SJ, Liao Z-X, Kao S-H, et al. Highly specific in-vivo gene delivery for p53-mediated apoptosis and genetic photodynamic therapies of tumour. Nat. Commun. 2015; 6
54. Cheng CJ, Bahal R, Babar IA, et al. MicroRNA silencing for cancer therapy targeted to the tumour microenvironment. Nature 2015; 518: 107-10.
55. Clark AJ, Davis ME. Increased brain uptake of targeted nanoparticles by adding an acid-cleavable linkage between transferrin and the nanoparticle core. Proc. Natl. Acad. Sci. U. S. A. 2015; 112: 12486-91.
56. Cui L, Cohen JL, Chu CK, et al. Conjugation Chemistry through Acetals toward a Dextran-Based Delivery System for Controlled Release of siRNA. J. Am. Chem. Soc. 2012; 134: 15840-8.
57. Lee K, Rafi M, Wang X, et al. In-vivo delivery of transcription factors with multifunctional oligonucleotides. Nat. Mater. 2015; 14: 701-6.
58. Lu Y, Hu Q, Lin Y, et al. Transformable liquid-metal nanomedicine. Nat. Commun. 2015; 6: 10066.
59. Ferrari M, Onuoha SC, Pitzalis C. Trojan horses and guided missiles: targeted therapies in the war on arthritis. Nat Rev Rheumatol 2015; 11: 328-37
60. Vandooren J, Opdenakker G, Loadman PM, et al. Proteases in cancer drug delivery. Adv. Drug Del. Rev. 2016; 97: 144-55
61. Huang S, Shao K, Liu Y, et al. Tumor-Targeting and Microenvironment-Responsive Smart Nanoparticles for Combination Therapy of Antiangiogenesis and Apoptosis. ACS Nano 2013; 7: 2860-71.
62. Van Rijt SH, Bölükbas DA, Argyo C, et al. Protease-Mediated Release of Chemotherapeutics from Mesoporous Silica Nanoparticles to ex-vivo Human and Mouse Lung Tumors. ACS Nano 2015; 9: 2377-89.
63. Thomas G. Furin at the cutting edge: From protein traffic to embryogenesis and disease. Nat. Rev. Mol. Cell. Biol. 2002; 3: 753-66.
64. Jiang T, Sun W, Zhu Q, et al. Furin-Mediated Sequential Delivery of Anticancer Cytokine and Small-Molecule Drug Shuttled by Graphene. Adv. Mater. 2015; 27: 1021-8.
65. Liu Z, Xiong M, Gong J, et al. Legumain protease-activated TAT-liposome cargo for targeting tumours and their microenvironment. Nat. Commun. 2014; 5.
66. Kuppusamy P, Li H, Ilangovan G, et al. Noninvasive imaging of tumor redox status and its modification by tissue glutathione levels. Cancer Res. 2002; 62: 307-12.
67. Dunn SS, Tian S, Blake S, et al. Reductively Responsive siRNA-Conjugated Hydrogel Nanoparticles for Gene Silencing. J. Am. Chem. Soc. 2012; 134: 7423-30.
68. Chang Y, Yang K, Wei P, et al. Cationic Vesicles Based on Amphiphilic Pillar[5]arene Capped with Ferrocenium: A Redox-Responsive System for Drug/siRNA Co- Delivery. Angew. Chem. Int. Ed. 2014; 53: 13126-30.
69. Waris G, Ahsan H. Reactive oxygen species: role in the development of cancer and various chronic conditions. Journal of carcinogenesis 2006; 5: 14
70. Cai H. Hydrogen peroxide regulation of endothelial function: origins, mechanisms, and consequences. Cardiovasc. Res. 2005; 68: 26-36.
71. Wang M, Sun S, Neufeld CI, et al. Reactive Oxygen Species-Responsive Protein Modification and Its Intracellular Delivery for Targeted Cancer Therapy. Angew. Chem. Int. Ed. 2014; 53: 13444-8.
72. Weinstain R, Savariar EN, Felsen CN, et al. In-vivo Targeting of Hydrogen Peroxide by Activatable Cell-Penetrating Peptides. J. Am. Chem. Soc. 2014; 136: 874-7.
73. Staff RH, Gallei M, Mazurowski M, et al. Patchy nanocapsules of poly(vinylferrocene)-based block copolymers for redox-responsive release. ACS Nano

2012; 6: 9042-9.
74. Zheng X, Wang X, Mao H, et al. Hypoxia-specific ultrasensitive detection of tumours and cancer cells in-vivo. Nat. Commun. 2015; 6
75. Thambi T, Deepagan VG, Yoon HY, et al. Hypoxia-responsive polymeric nanoparticles for tumor-targeted drug delivery. Biomaterials 2014; 35: 1735-43
76. Zhou Y, Tozzi F, Chen J, et al. Intracellular ATP levels are a pivotal determinant of chemoresistance in colon cancer cells. Cancer Res. 2012; 72: 304-14
77. Mo R, Jiang T, Sun W, et al. ATP-Responsive DNA-Graphene Hybrid Nanoaggregates for Anticancer Drug Delivery. Biomaterials 2015; 50: 67-74.
78. Lai J, Shah BP, Zhang Y, et al. Real-Time Monitoring of ATP-Responsive Drug Release Using Mesoporous-Silica-Coated Multicolor Upconversion Nanoparticles. ACS Nano 2015; 9: 5234-45.